New Research Proposal to Jefferson Lab PAC 33

Transverse spin effects in SIDIS at 6 GeV with transversely polarized target using the CLAS Detector

H. Avakian[1], P. Bosted[1], S. Boyarinov, V.D. Burkert, A. Deur, L. Elouadrhiri, R. Ent, D. Gaskell, T. Kageya, V. Koubarovsky, M. Lowry, A. Sandorfi, Yu. Sharabian, S. Stepanyan, X.Wei
Jefferson Lab, Newport News, VA 23606, USA

N. Makins[1,2]
University of Illinois at Urbana-Champaign, 1110 West Green St. Urbana, IL 61801, USA

P. Rossi[1], E. De Sanctis, M. Aghasyan, L. Hovsepyan, M. Mirazita, and S. Anefalos Pereira
LNF INFN, Frascati, I00044, Rome Italy

K. Hafidi[1], J. Arrington, L. El Fassi, D. F. Geesaman, R. J. Holt,
D. H. Potterveld, P. E. Reimer, P. Solvignon
Argonne National Lab, Argonne, IL 60439, USA

J. Ball, M. Garçon, M. Guidal, A. Kotzinian, M. Mac Cormick, S. Niccolai, F. Sabatié
IPNO (Orsay), SPhN (Saclay) France

M. Amarian, G. Dodge, S.E. Kuhn
Old Dominion University, Norfolk, VA 23529, USA

R. Niyazov, P. Stoler
Rensselaer Polytechnic Institute, Troy, NY 12181, USA

D. Ireland, R. Kaiser, I. Lehmann, K. Livingston, D. Protopopescu, G. Rosner, B. Seitz
Univ. of Glasgow, Glasgow G12 8QQ, UK

P. Dalpiaz, M. Contalbrigo, L. Pappaladro, F. Giordano
University of Ferrara, Via Paradiso, I-44100, Ferrara, Italy

A. D'Angelo, A. Fantini, D. Franco, D. Moricciani, C. Schaerf, V. Vegna
Dipartimento di Fisica, Universita' di Roma Tor Vergata,
INFN Sezione di Roma Tor Vergata, Via della Ricerca Scientifica 1- I00133, Rome, Italy

A. Biselli
Fairfield University, Fairfield CT 06824, USA

K. Joo, N. Markov, M. Ungaro, B. Zhao
University of Connecticut, Storrs, CT 06269, USA

[1]Co-spokesperson
[2]Contact person

S. Kuleshov, O. Pogorelko
Institute of Theoretical and Experimental Physics, Moscow, 117259, Russia

E.N. Golovach, G.V. Fedotov, B.S. Ishkhanov, E.L. Isupov, V.I. Mokeev, N.V. Shvedunov
Skobeltsyn Institute of Nuclear Physics and Physics Department at Moscow State University
19899 Vorob'evy gory, Skobeltsyn Nuclear Physics Institute at Moscow State University, Moscow, Russia

D. Crabb, S.Liuti, L.C. Smith
UVA, Charlottesville, VA 22904,USA

X.Jiang
Los Alamos National Laboratory, Los Alamos, NM 87545, USA

G. Huber, Dept. of Physics, Univ. of Regina, Regina, SK S4S0A2, Canada

M. Anselmino, B. Parsamyan, A. Prokudin
Università di Torino and INFN, Sezione di Torino, Via P. Giuria 1, I-10125 Torino
P. Schweitzer, Ruhr-Universitat Bochum, 44780, Bochum Germany
A. Metz Temple University 1900 N. 13th St.Philadelphia, PA 19122, 6082, USA
L. Gamberg, Penn State Berks, Reading, PA 19610, USA
G.R. Goldstein, Tufts University, Medford, MA 02155, USA

Abstract

We propose to study the spin azimuthal asymmetries in semi-inclusive DIS (SIDIS) using the CEBAF 6 GeV polarized electron beam, a transversely polarized HD-Ice target, and the CEBAF Large Acceptance Spectrometer (CLAS). The main focus of the experiment will be the measurement of the transverse target single-spin asymmetries (TTSA) in the reaction $ep^{\uparrow} \rightarrow e\pi X$. Three main observable asymmetries provide access to the Sivers function describing the unpolarized quarks and transversity and "pretzelosity" distributions describing transversely polarized quarks in the transversely polarized nucleon. The expected asymmetries from the leading-order calculations are in the range of 2 to 10%, depending on the kinematics and on the Transverse Momentum Dependent (TMD) parton distribution models used. The x, z and P_T dependences of the TTSAs will be studied in a wide range of kinematics. In addition, transverse spin dependent double spin asymmetries (TDSA) for $\vec{e}p^{\uparrow} \rightarrow e\pi X$ will be measured simultaneously, giving access to distribution of longitudinally polarized quarks in the transversely polarized nucleon. This experiment will also provide important information of sub-leading order parton distributions and in particular extend significantly the (x, Q^2) range of precision measurements of g_2.

A total of 45 days of new beam time is requested for this experiment.

Contents

1 Introduction

The spin structure of the nucleon has been of particular interest since the EMC [1] measurements implied that the helicity of the constituent quarks account for only a fraction of the nucleon spin. The so-called "spin puzzle" was subsequently confirmed by a number of other experiments at CERN [2], SLAC [3, 4], HERA [5, 6], and JLab [7]. Possible interpretations of this result include the contribution of the orbital momentum of quarks and significant polarization of either the strange sea (negatively polarized) or gluons (positively polarized). The contributions to the sum rule for the total helicity of the nucleon include heuristically the following:

$$\frac{1}{2} = \frac{1}{2}\sum_q (\Delta q^{val} + \Delta q^{sea}) + L_z^{val} + L_z^{sea} + L_z^{glue} + \Delta G, \tag{1}$$

where Δq, L_z, and ΔG are respectively the quark helicity, the orbital angular momentum of all partons, and the gluon helicity.

Present knowledge about the spin structure of the nucleon, described by parton distribution functions comes mainly from polarized deep inelastic scattering (DIS). The polarization of the individual flavors and anti-flavors were mainly studied using fits to the inclusive data. Inclusive DIS is sensitive to only the squared charges of the partons, and requires additional assumptions (*e.g.* an SU(3) symmetric sea), which lead to model dependence. Semi-inclusive deep inelastic scattering (SIDIS) studies, for which a hadron is detected in coincidence with the scattered lepton allows so-called "flavor tagging", provide more direct access to contributions from various quarks. In addition, they give access to the transverse momentum distributions of quarks, not accessible in inclusive scattering. Azimuthal distributions of final state particles in semi-inclusive deep inelastic scattering provide access to the orbital motion of quarks and play an important role in the study of transverse momentum distributions of quarks in the nucleon.

Significant progress has been made recently in understanding the role of partonic initial and final state interactions [8, 9, 10]. The interaction between the active parton in the hadron and the spectators leads to gauge-invariant transverse momentum dependent (TMD) parton distributions [8, 9, 10, 11, 12, 13]. Furthermore, QCD factorization for semi-inclusive deep inelastic scattering at low transverse momentum in the current-fragmentation region has been established in Refs. [14, 15]. This new framework provides a rigorous basis to study the TMD parton distributions from SIDIS data using different spin-dependent and independent observables. TMD distributions (see Table 1) describe transitions of a nucleon with one polarization in the initial state to a quark with another polarization in the final state.

The diagonal elements of the table are the momentum, longitudinal and transverse spin distributions of partons, and represent well-known parton distribution functions related to the square of the leading-twist, light-cone wave functions. Off-diagonal elements require non-zero orbital angular momentum and are related to the wave

N/q	U	L	T
U	$\mathbf{f_1}$		$h_1^\perp$
L		$\mathbf{g_1}$	$h_{1L}^\perp$
T	$f_{1T}^\perp$	g_{1T}	$\mathbf{h_1}$ $h_{1T}^\perp$

Table 1: Leading-twist transverse momentum-dependent distribution functions. U, L, and T stand for transitions of unpolarized, longitudinally polarized, and transversely polarized nucleons (rows) to corresponding quarks (columns).

function overlap of L=0 and L=1 Fock states of the nucleon [16]. The TMDs $f_{1T}^\perp$ and $h_1^\perp$, which are related to the imaginary part of the interference of wave functions for different orbital momentum states and are known as the Sivers and Boer-Mulders functions [17, 18, 19, 20, 9, 10, 11], describe unpolarized quarks in the transversely polarized nucleon and transversely polarized quarks in the unpolarized nucleon respectively. They vanish at tree-level in a T-reversal invariant model (T-odd) and can only be non-zero when initial or final state interactions cause an interference between different helicity states. These functions parameterize the correlations between the transverse momentum of quarks and the spin of a transversely polarized target or the transverse spin of the quark, respectively. They require both orbital angular momentum, as well as non-trivial phases from the initial/final state interaction, that survive in the Bjorken limit. Experimental results on the Sivers functions for up and down quarks so far are consistent with a heuristic model of up and down quarks orbiting the nucleon in opposite directions.

The impact parameter space displacement of unpolarized quarks in the transversely polarized proton is described by the Generalized Parton Distribution E (GPD-E) [21], and has recently been calculated in lattice QCD [22, 23]. These results suggest on the basis of Burkard's model discussed above, that the Sivers functions are significant. Moreover, consistent with large N_C predictions, the displacement of u and d quarks was found to be in opposite directions, indicating different signs for the Sivers functions for u and d quarks (Fig. 1).

Similar quantities arise in the hadronization process. One particular case is the Collins T-odd fragmentation function $H_1^\perp$ [24] describing fragmentation of transversely polarized quarks into unpolarized hadrons. Parton model analysis [25, 26, 27, 28] of sub-leading single-spin asymmetries which were observed at HERMES [29, 30, 31, 32] and CLAS [33] led to the introduction of new twist-3 T-odd distribution functions [28, 34, 35].

The off-diagonal TMD distributions for transversely polarized quarks arise from interference between amplitudes with left- and right-handed polarization states, and only exist because of chiral symmetry breaking in the nucleon wave function in QCD. Their study therefore provides a new avenue for probing the chiral nature of the partonic structure of hadrons. The universality of the TMD correlation functions has

been proven, resulting in a sign change for two T-odd TMD distributions between Drell-Yan and DIS [9, 15], an exciting prediction that has to be confirmed by future experiments.

We propose a high luminosity (5×10^{33} cm^{-2}s^{-1}) measurement of transverse target single spin asymmetries in SIDIS using the CLAS in Hall B with a 6 GeV longitudinally polarized electron beam and the transversely polarized HD-Ice target. The proposed measurements are essential for the study of transverse momentum dependent distributions, and when combined with already approved CLAS measurements with unpolarized and longitudinally polarized targets will constrain all chiral-odd leading twist TMDs in the range of Q^2 from 1 to 4 GeV^2, and x_B from 0.15 to 0.55. The same measurement will also provide important information on different sub-leading distribution functions [36, 37]. The main goal of this proposal will be the study of the x and P_T dependences of the target SSAs (TTSAs).

The CLAS detector provides a unique opportunity to perform the measurements over a wide range of kinematics with a single experiment.

2 Theory and motivation

In recent years, semi-inclusive deep inelastic scattering (SIDIS) has emerged as a powerful tool to probe nucleon structure through measurements of single spin asymmetries (SSAs) [29, 38, 39]. In contrast to inclusive deep inelastic lepton-nucleon scattering where transverse momentum is integrated out, these processes are sensitive to transverse momentum scales on the order of the intrinsic quark momentum. Measurements of SSAs in SIDIS provide access to a list of novel physics observables including transversity (h_1) [40, 41], and the time-reversal odd Sivers distribution function ($f_{1T}^{\perp}$) [17, 19, 8, 9, 10].

The SIDIS cross section at leading twist has eight contributions related to different combinations of polarization states of the incoming lepton and the target nucleon [14]:

$$\begin{aligned}\frac{d\sigma}{dxdydz_h d^2\vec{P}_T} &= \frac{4\pi\alpha_{\rm em}^2 s}{Q^4}(1-y+y^2/2)xF_{UU}^{(1)} - (1-y)x\cos(2\phi)F_{UU}^{(2)} \\ &+\lambda S_L y(1-y/2)xF_{LL} + S_L(1-y)x\sin(2\phi)F_{UL} \\ &+|S_T|(1-y+y^2/2)x\sin(\phi-\phi_S)F_{UT}^{(1)} \\ &+|S_T|(1-y)x\sin(\phi+\phi_S)F_{UT}^{(2)} \\ &+\lambda|S_T|y(1-y/2)x\cos(\phi-\phi_S)F_{LT} \\ &+\tfrac{1}{2}|S_T|(1-y)x\sin(3\phi-\phi_S)F_{UT}^{(3)}] \end{aligned} \quad (2)$$

The kinematic variables x, y are defined as: $x = Q^2/2(Pq)$, and $y = (Pq)/(Pl)$. The $q = l - l'$ is the momentum of the virtual photon, $Q^2 = -q^2$, ϕ is the azimuthal

angle between the scattering plane formed by the initial and final momenta of the electron and the production plane formed by the transverse momentum of the observed hadron, P_T, and the virtual photon (Fig. 2), ϕ_S is the azimuthal angle of the transverse spin in the scattering plane, P and P_T are the initial nucleon momentum and final hadron transverse momentum, respectively. The subscripts in $F_{UT,UL,LT}$, specify the beam (first index) and target polarizations (U, L, T for unpolarized, longitudinally and transversely polarized targets, and U, L for unpolarized and longitudinally polarized beam), S_L and S_T are the longitudinal and transverse components of the target polarization with respect to the direction of the virtual photon.

Structure functions factorize into TMD parton distribution and fragmentation functions, and soft and hard parts [14]. For example the $F_{UT}^{(2)}$ can be written as

$$F_{UT}^{(2)} = \int \frac{\vec{p}_\perp \cdot \hat{\vec{P}}_T}{M} \times h_1(x, k_\perp)\, H_1^\perp(z, p_\perp)\, S(\vec{\lambda}_\perp) H_{UT}^{(2)}\left(Q^2\right) . \tag{3}$$

The hard factor, H_{UT}, is calculable in pQCD, and the soft factor $S(\vec{\lambda}_\perp)$ comes from soft gluon radiation and is defined by a matrix element of Wilson lines in the QCD vacuum [14]. The integral symbol represents integration over transverse momentum of initial, $k_\perp$, and scattered $p_\perp$ partons and the soft gluon momentum $\vec{\lambda}_\perp$ [42]. Distribution (h_1) and fragmentation ($H_1^\perp$) functions involved, depend on fractions of the proton momentum carried by the struck quark, x, and the virtual photon momentum carried by the final state hadron z and also the corresponding transverse momenta $k_\perp$, and $p_\perp$.

2.1 Transversely polarized target

For transversely polarized target, several azimuthal asymmetries already arise at leading order. Four contributions related to the corresponding distribution functions were investigated in Refs. [24, 43, 44, 8, 10, 45]:

$$\sigma_{LT}^{\cos\phi} \propto \lambda_e S_T y(1-y/2)\cos(\phi-\phi_S)\sum_{q,\bar{q}} e_q^2 x g_{1T}^q(x) D_1^q(z), \tag{4}$$

$$\begin{aligned}\sigma_{UT}^{\sin\phi} &\propto S_T(1-y)\sin(\phi+\phi_S)\sum_{q,\bar{q}} e_q^2 x h_1(x) H_1^{\perp q}(z) \\ &+ S_T(1-y+y^2/2)\sin(\phi-\phi_S)\sum_{q,\bar{q}} e_q^2 x f_{1T}^{\perp q}(x) D_1^q(z) \\ &+ S_T(1-y)\sin(3\phi-\phi_S)\sum_{q,\bar{q}} e_q^2 x h_{1T}^{\perp q}(x) H_1^{\perp q}(z),\end{aligned} \tag{5}$$

where y defines the fraction of electron momentum carried by the virtual photon. $D_1^q(z)$ and $H_1^{\perp q}(z)$ are the spin-independent and spin-dependent fragmentation functions.

The leading-twist transversity distribution h_1 [40, 41] and its first moment, the tensor charge, are as fundamental for understanding of the spin structure of the nucleon as are the helicity distribution g_1 and the axial vector charge. The transversity distribution h_1 is charge conjugation odd. It is chirally odd, and there is no gluon transversity in the nucleon. For non-relativistic quarks it is equal to the helicity distribution g_1. Thus, it probes the relativistic nature of quarks and it has a very different Q^2 evolution than g_1. The tensor charge is reliably calculable in lattice QCD with $\delta\Sigma = \sum_f \int_0^1 dx(h_1^f - h_1^f) = 0.562 \pm 0.088$ at Q^2=2 GeV^2, which is twice as large as the value of axial charge [46]. A similar quantity ($\delta\Sigma \approx 0.6$) was obtained in the effective chiral quark soliton model [47].

A detailed study of x, y, z, and P_T dependences as a function of the azimuthal angle ϕ will allow the separation of contributions from different mechanisms.

The data from CLAS with a transversely polarized target focusing on TTSAs, combined with data from unpolarized and longitudinally polarized targets, will provide a complete set of measurements required for the separation of all eight leading-twist TMDs, providing important information on spin-orbit correlations.

It is important to note that both π^+ and π^- azimuthal moments may have significant contributions from exclusive vector meson production. The fraction of π^+ in the single pion sample, coming from exclusive ρ^0 decays, is somewhat less but still significant at large z and in particular for small x. The two pion data from this experiment will allow us to extract exclusive two pion asymmetries and estimate their contribution to the single pion SSA.

A full program to extract TMDs from measurements requires coverage of a large kinematic range in x, z, and P_T along with measurements of all three final state pions together with the use of polarized beam and polarized targets (both longitudinal and transverse polarizations).

2.2 Relations between GPDs and TMDs

The TMDs define the probability density of finding a (polarized) quark with a certain polarization with longitudinal momentum fraction x and transverse momentum k_T inside polarized and unpolarized nucleons. For example, the probability of finding an unpolarized quark with longitudinal momentum fraction x and transverse momentum $\vec{k}_T$ inside a transversely polarized target is given by:

$$\Phi^q(x, \vec{k}_T; S) = f_1^q(x, \vec{k}_T^2) - \frac{(\hat{P} \times k_T) S_T}{M} f_{1T}^{\perp q}(x, \vec{k}_T^2)\,, \tag{6}$$

Similarly to the TMDs in momentum space, the impact parameter dependent generalized parton distributions (GPDs) [48, 49, 50, 51] have a probability interpretation, too. The impact parameter dependent GPDs [52][3] are defined as the two-dimensional

[3] also a subject of a new proposal [53]

Fourier transform of the GPD (for $\xi = 0$), with respect to transverse momentum transfer, $\mathbf{\Delta}_\perp$, describing the distributions of quarks with longitudinal momentum fraction x over the transverse distance, $\vec{b}_T$, from the center of the nucleon (impact parameter). The integral of this spatial distribution over $\vec{b}_T$ gives the total parton density at a longitudinal momentum fraction x. This 1+2-dimensional "mixed" momentum and coordinate representation corresponds to a set of "tomographic images" of the quark distribution in the nucleon at fixed longitudinal momentum, x.

Quark density distributions in the transverse plane for different combinations of transverse spin of proton and quark [23] are shown in Fig. 1.

The probability density of finding an unpolarized quark with longitudinal momentum fraction x at transverse position $\vec{b}_T$ inside a transversely polarized nucleon is given by:

$$\mathcal{F}^q(x, \vec{b}_T; S) = \mathcal{H}^q(x, \vec{b}_T^2) + \frac{(\hat{P} \times b_T) S_T}{M} \left(\mathcal{E}^q(x, \vec{b}_T^2) \right)' , \tag{7}$$

where S parametrizes all possible combinations of the helicities λ and λ' as described in Refs. [54, 55]. The GPDs $\mathcal{H}^q$ and $\mathcal{E}^q$ are the Fourier transformed GPDs H^q and E^q, respectively, and the prime denotes the first derivative with respect to $\vec{b}_T^2$.

The respective structures of the density distributions in Eqs. (6) and (7) are identical after exchanging the impact parameter $\vec{b}_T$ and the transverse parton momentum $\vec{k}_T$. This, together with the similar probability interpretations, inspires the assumption that there might exist some relations between these two objects. The following set of possible relations, has been proposed [54]:

$$\begin{aligned} \mathcal{H}^{q/g} \;&\leftrightarrow\; f_1^{q/g} , \qquad & \tilde{\mathcal{H}}^{q/g} \;&\leftrightarrow\; g_{1L}^{q/g} , \\ \left(\mathcal{H}_T^q - \tfrac{\vec{b}_T^2}{M^2} \Delta_b \tilde{\mathcal{H}}_T^q \right) , \;&\leftrightarrow\; \left(h_{1T}^q + \tfrac{\vec{k}_T^2}{2M^2} h_{1T}^{\perp q} \right) \end{aligned} \tag{8}$$

$$\begin{aligned} \left(\mathcal{E}^{q/g} \right)' \;&\leftrightarrow\; -f_{1T}^{\perp q/g} , \qquad & \left(\mathcal{E}_T^q + 2\tilde{\mathcal{H}}_T^q \right)' \;&\leftrightarrow\; -h_1^{\perp q} , \\ \left(\tilde{\mathcal{H}}_T^q \right)'' \;&\leftrightarrow\; \tfrac{1}{2} h_{1T}^{\perp q} \end{aligned} \tag{9}$$

These relations may have very interesting phenomenological implications [56, 54, 21, 57, 55]. One particular example is the TMD describing transversely polarized quarks in the transversely polarized nucleon, chirally odd tensor correlation $h_{1T}^\perp$. Studies of the shape of the proton indicate [58, 59], that for the transversely polarized quarks in the transversely polarized nucleon the shape of the nucleon reminds a pretzel. The distribution of transversely polarized quarks is described by the TMD $h_{1T}^\perp$ and its magnitude will thus, be related to "pretzelosity" of the proton [58].

It was shown that in some simple spectator models (a scalar diquark spectator model of the nucleon and a quark target model in perturbative QCD) all relations actually hold to lowest order in perturbation theory [55].

While the Eq. (8) represents a well known property of the GPDs and TMDs to reduce to the same forward parton distributions, other relations [56, 57, 55] provide non-trivial links between corresponding moments of GPDs and TMDs. For the distribution describing transversely polarized quarks in the transversely polarized nucleon that relation is given by:

$$\int d^2\vec{b}_T\, \vec{b}_T^{\,2} \left(\tilde{\mathcal{H}}_T^q(x, \vec{b}_T^{\,2})\right)'' = \int d^2\vec{k}_T\, \vec{k}_T^{\,2}\, \tfrac{1}{2} h_{1T}^{\perp q}(x, \vec{k}_T^{\,2}) \tag{10}$$

with similar forms for the other relations. Global analysis of hard exclusive (accessing GPDs) and semi-inclusive processes (accessing TMDs) will provide tests of those relations.

2.3 Present Experimental Results on Spin-Azimuthal Asymmetries

During the last few years, first results on transverse SSAs have become available [38, 39]. HERMES measurements for the first time directly indicated significant azimuthal moments generated both by Collins (Fig. 3) and Sivers (Fig. 4) effects.

The extraction of the transversity from $A_{UT}^{\sin(\phi+\phi_S)}$ requires parameterizations for the unpolarized distribution functions along with approximations for the essentially unknown polarized Collins fragmentation function $H_1^\perp$. The Collins function for pions was calculated in a chiral invariant approach at a low scale [60]. It was shown that at large z the function rises much faster than previously predicted [25, 61] in the analysis using the HERMES data on target SSA. Significant asymmetry was measured recently by Belle [62] indicating that the Collins function is indeed large. The first extraction of the transversity distribution has been carried out recently [63] combining e^+e^- and semi-inclusive DIS from HERMES [38] and COMPASS [39, 64]. The statistics, however, are not enough to make statistically significant predictions in the valence region, where the effects are large. The effects related to orbital motion of quarks and in particular correlations of spin and transverse momentum of quarks play more important role in the valence region. It was shown that spin-orbit correlations may lead to significant contribution to partonic momentum and helicity distributions [65] in large-x limit.

Significantly higher statistics from CLAS data, especially in the large x region, will enable the extraction of the x, z and P_T dependences for different azimuthal moments in a wide kinematic range allowing the source of the observed SSA to be revealed and will allow extraction of the underlying distribution functions.

The Sivers contribution, being leading twist, is expected to survive at higher Q^2 and that can be tested in future at the large Q^2 accessible with `CLAS12`. At large transverse momentum, *i.e.* $P_{h\perp} \gg \Lambda_{\rm QCD}$, the transverse-momentum dependence of the various factors in the factorization formula [14] may be calculated from pertur-

bative QCD. Following arguments in Ji-Qiu-Vogelsang-Yuan [66], the $\sin(\phi - \phi_S)$ azimuthal asymmetry has the following behavior at $\Lambda_{\rm QCD} \ll P_{h\perp} \ll Q$,

$$\langle \sin\phi - \phi_S \rangle|_{P_{h\perp} \gg \Lambda_{\rm QCD}} \propto \frac{1}{P_{h\perp}} \ . \tag{11}$$

The above result holds also when the transverse momentum is compatible with the large-scale Q. Measurement of the P_T dependence of the Sivers-asymmetry will, thus, check of the predictions of a unified description of SSA by Ji and collaborators [14, 66] and will study the transition from a non-perturbative to a perturbative description. The Sivers asymmetry for semi-inclusive deep inelastic scattering in the kinematic regions of CLAS is predicted to be significant ($\sim$ 10% at large P_T) and tends to be larger in the large-x and large-z region. Measurement of the P_T-dependence of the Sivers asymmetry provide access to the transverse momentum dependence of the Sivers TMD and its moments. This would allow one, in particular, to determine the first moment of the Sivers function:

$$f_{1T}^{\perp(1)}(x) = \int d^2\vec{k}_T \, \frac{\vec{k}_T^2}{2M^2} \, f_{1T}^{\perp(1)}(x, \vec{k}_T^2) \tag{12}$$

This moment has a direct connection to so called soft gluon pole matrix elements [67, 13, 55], and as a consequence one may also get a direct connection to the large single spin asymmetries already observed in, for instance, $p^\uparrow p \to \pi X$ at Fermilab [68] and at RHIC [69]. Making such a cross check is indispensable if one wants to decide whether we have reached a proper understanding of various transverse single spin phenomena in semi-inclusive reactions by means of perturbative QCD.

The combined analysis of the future CLAS data on A_{UT} and of the previous HERMES and COMPASS measurements in the small-x domain, will provide information on the Sivers function, shedding light on the correlations between transverse spin and transverse momenta of quarks.

The transversely polarized target measurements also provide access to the leading-twist TMD $g_{1T}^q(x)$ appearing in convolution with the unpolarized fragmentation function $D_1^q(z)$ in a $\cos\phi$ moment of the cross section. Significant asymmetries which were predicted recently for CLAS kinematics [70] provide access also to $g_{1T}^q(x)$, describing longitudinally polarized quarks in the transversely polarized nucleon (see Fig. 5).

Measured single and double spin asymmetries for all pions in a large range of kinematic variables (x, Q^2, z, $P_\perp$, and ϕ) combined with measurements with unpolarized targets will provide detailed information on the flavor and polarization dependence of the transverse momentum distributions of quarks in the valence region, and in particular, on the x, z, and $P_\perp$ dependence of the leading TMD parton distribution functions of u and d quarks. Such measurements across a wide range of x, Q^2, and P_T would allow for detailed tests of QCD dynamics in the valence region complementing the information obtained from inclusive DIS. They would also serve as novel tools

for exploring nuclear structure in terms of the quark and gluon degrees of freedom of QCD.

Combination of all 3 target polarizations opens access to study of single- and double-spin asymmetries, involving essentially unexplored chiral-odd and time-odd distributions functions. The list includes transversity [40, 41], Sivers [17, 8, 9, 10], "pretzelosity" [43], and Collins [24] functions, providing detailed information on the quark transverse momentum and spin correlations [24, 44, 43, 20, 71].

2.4 Current Fragmentation in SIDIS at 6GeV

Important issues at low beam energies are the separation of current and target fragmentation regions and the presence of factorization when the quark scattering process and the fragmentation process factorize, and the fragmentation functions depend only on the fractional energy, z. At low beam energies in DIS the current fragmentation region (CFR) is contaminated with events coming from the target fragmentation region (TFR). A simple graphical representation of different regions as a function of relevant kinematic variables z, x_F and η is available from Mulders and collaborators. At low z and x_F and rapidities $\eta < 1$ (Fig. 6) a significant overlap of current and target fragmentation regions is expected .

Factorization in the z-distributions of pions was studied using the the 6 GeV data from CLAS[72] and Hall-C[73] experiments. No significant dependence within statistical uncertainties was observed in z-distributions for different values of x available to the experiment.

2.4.1 MC studies and factorization

The kinematic coverage in x and missing mass of the $e'\pi$ system (Fig. 7) shows there are a significant number of events in the kinematic region where the remnant mass (M_X) after the release of a fast pion is relatively low (Fig. 8). Apart from the nucleon, the Δ also shows up in the distributions over the missing mass, raising a question on how well events in DIS kinematics, defined by standard DIS cuts $Q^2 > 1$ GeV^2 and $W^2 > 4$ GeV at JLab energies, could be described using the DIS formalism.

Studies performed at beam energies as low as 4 GeV[33] showed no significant dependence on x, both for pion multiplicities and beam SSAs, as a function of z within statistical uncertainties ($10 - 15\%$). A variety of possible observables to test the factorization is provided when measuring single and double polarized asymmetries as a function of x or z in different bins of z and x respectively.

Different kinematical distributions from PEPSI-MC were compared with data (Figures 9,10), showing good agreement for π^+ SIDIS data with LUND-MC at 6 GeV. Good description of data with LUND-MC is also important for future analysis of SSAs.

Various tests of the validity of factorization of semi-inclusive electroproduction cross section into a product of quark distribution functions and favored and unfa-

vored fragmentation functions were performed using spin-dependent and independent observables at JLab at 6 GeV.

Studies of the proton to deuteron ratio of the the sum and difference of π^+ and π^- production rates were performed at Hall-C. In LO QCD and ignoring sea quark contributions, fragmentation functions cancel in both of these ratios, which should therefore be independent of z and $P_\perp$, and have the x-dependence observed in inclusive scattering determinations of u and d quark distribution functions. It was shown that these ratios for $x = 0.3$ indeed are independent of z up to $z = 0.7$.

2.5 Inclusive Structure Function g_2

Measurements of the inclusive double spin asymmetry A_{LT} will be obtained as a bonus from the present proposal. They are of particular interest due to their large sensitivity to the $g_2(x, Q^2)$ structure function. We plan to use a fit to world data on the longitudinal double spin asymmetry A_{LL} to extract g_2 for both the proton and deuteron. The kinematic range covered will be large: $1.1 < W < 3.2$ GeV, and $0.5 < Q^2 < 5$ GeV^2. One of the principal physics interests is that, after correction for a kinematic twist-two contribution which only involves the well-known g_1 structure function, the resulting $\bar{g}_2$ is sensitive to twist-three contributions from quark-gluon correlations in the nucleon [74]. The third moment of this twist-three contribution (known as $\bar{d}_2$) is of particular interest, because it can and has been calculated in rigorous treatments of QCD such as lattice models [75, 76]. Experimentally, it is important to study the Q^2 dependence of both $\bar{g}_2$ and $\bar{d}_2$, in order to separate the twist-3 behavior (approximately proportional to $1/\sqrt{Q^2}$) from higher twist contributions (proportional to $1/Q^2$, $1/Q^4$, ...). Since models predict very different values of $\bar{d}_2$ for the proton and neutron, it is important to make precision measurements of both the proton and deuteron. The neutron results extracted from the proton and deuteron can be compared with the extensive g_2 measurements from Hall A [77, 78] using a ^{3}He target. Nuclear corrections can be important in the extraction of neutron g_2 from ^{3}He at high x and low to moderate Q^2, which is precisely the range accessible in the present proposal.

From a pragmatic point of view, precise measurements of g_2 are of vital importance to the extraction of A_1 and g_1 from the A_{LL} measurements of Eg1 [79] and Eg4 at CLAS. At present, the systematic error due to the lack of precision measurements of g_2 is one of the dominant errors in this extraction, especially for the virtual photon asymmetry A_1. This is of particular importance for reliably obtaining the polarisibility integral $\gamma_0(Q^2) = \int x^2 F_1(x, Q^2) A_1(x, Q^2) dx$. Data over a wide kinematic range are also needed for precise evaluations of radiative corrections.

Another quantity that will extracted from this presently proposed experiment is the forward spin polarizability δ_{LT}. It can be formed using higher moments of g_1 and

g_2 and the following sum rule [80, 81]:

$$\begin{aligned}\delta_{LT}(Q^2) &= (\frac{1}{2\pi^2})\int_{\nu_0}^{\infty}\frac{\kappa(\nu,Q^2)}{\nu}\frac{\sigma_{LT}(\nu,Q^2)}{Q\nu^2}d\nu \\ &= \frac{16\alpha M^2}{Q^6}\int_0^{x_0}x^2\Big[g_1(x,Q^2)+g_2(x,Q^2)\Big]dx. \qquad (13)\end{aligned}$$

There are two interesting fundamental QCD predictions to study: a) in the high Q^2 limit, does $\delta_{LT}(Q^2) \to \frac{1}{3}\gamma_0(Q^2)$?; b) do $Q^6\delta_{LT}(Q^2)$ and $Q^6\gamma_0(Q^2)$ scale with Q^2? Combined with other world data, the data from the present proposal will allow such studies in the range $0.5 < Q^2 < 5$ GeV^2 with good precision.

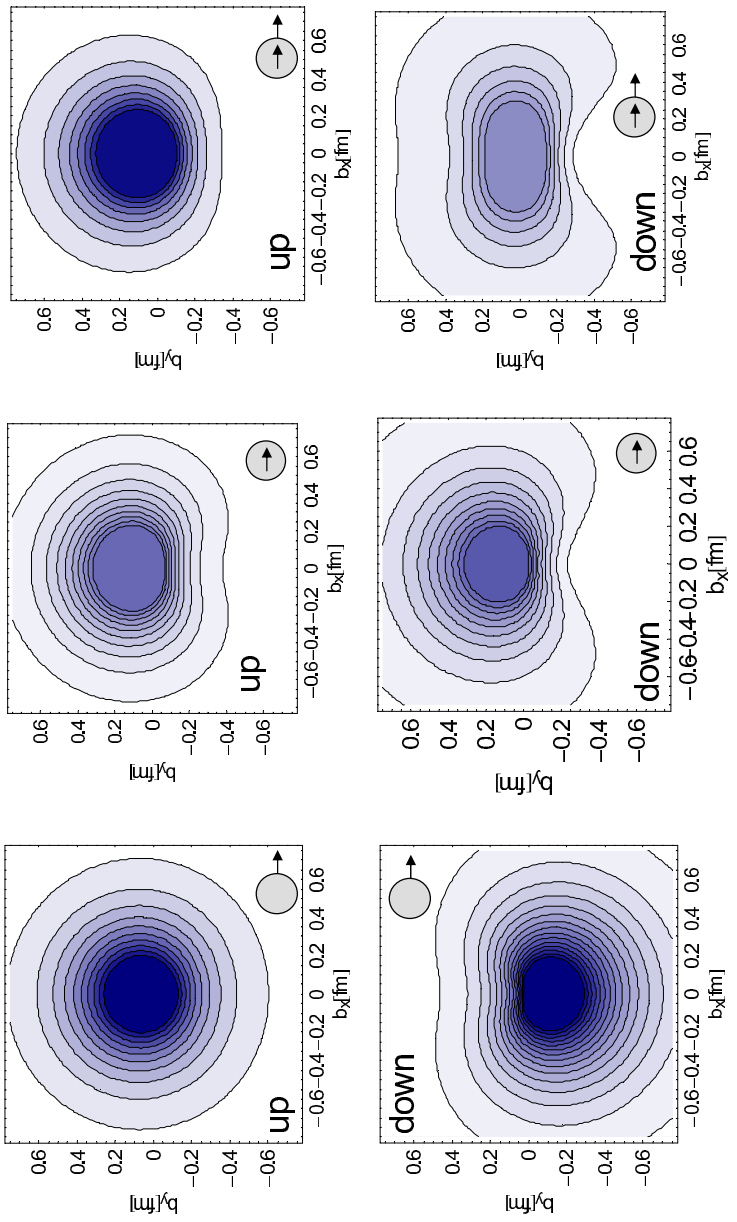

Figure 1: Density distributions for different combinations of proton and quark spin. Outer arrows show the proton, and inner arrows show the quark transverse polarizations

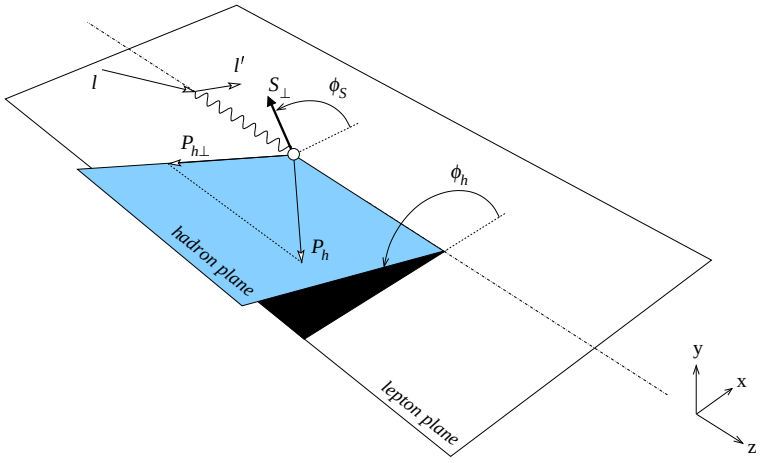

Figure 2: The SIDIS kinematics

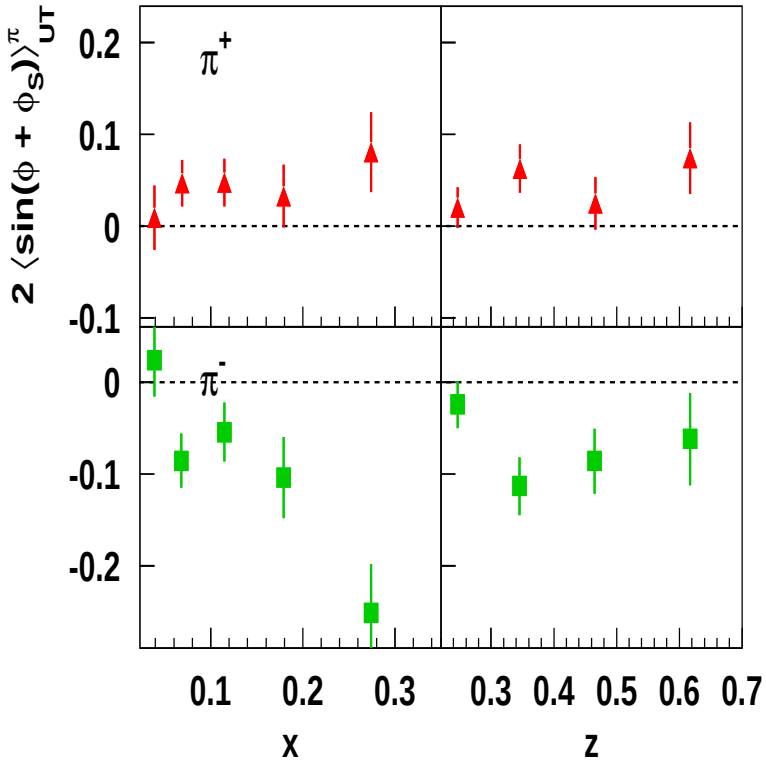

Figure 3: Transverse spin asymmetry from the Collins effect ($A_{UT}^{\sin(\phi+\phi_S)}$) in single π production from HERMES

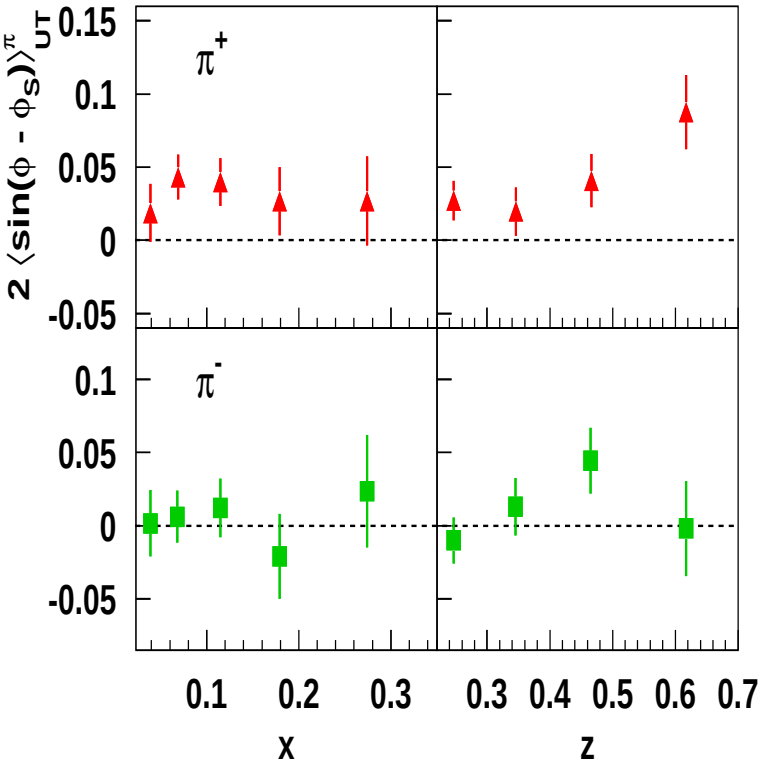

Figure 4: Transverse spin asymmetry from the Sivers effect ($A_{UT}^{\sin(\phi-\phi_S)}$) in single π production from HERMES

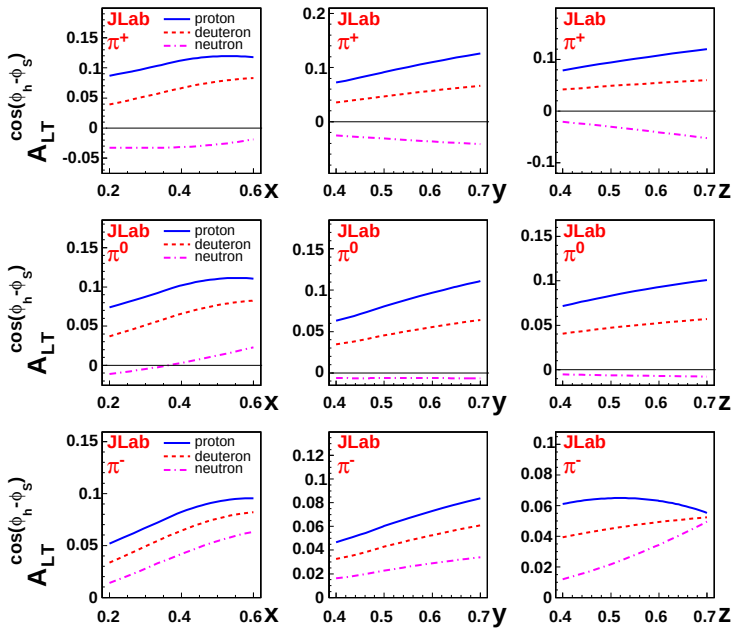

Figure 5: Predicted dependence of $A_{LT}^{\cos(\phi-\phi_S)}$ on x, y and z with $|\mathbf{P}_{T,min}| = 0.5$ GeV/c for CLAS at 6 GeV.

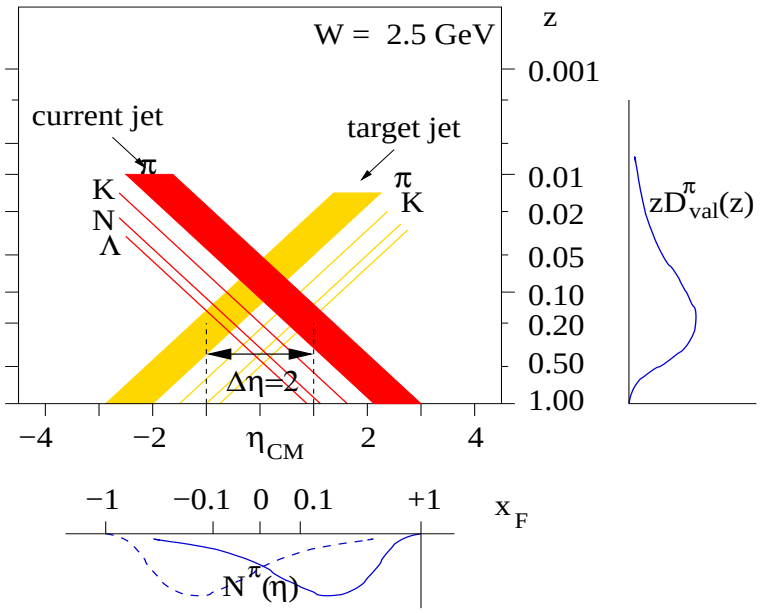

Figure 6: The SIDIS kinematics at $W = 2.5$ GeV. The kinematic variables are defined as follows: $z = \frac{E_h}{\nu}$, $x_F = \frac{p^*_L}{p^*_{Lmax}}$ and $\eta = \frac{1}{2} ln \frac{E+p^*_L}{E-p^*_L}$.

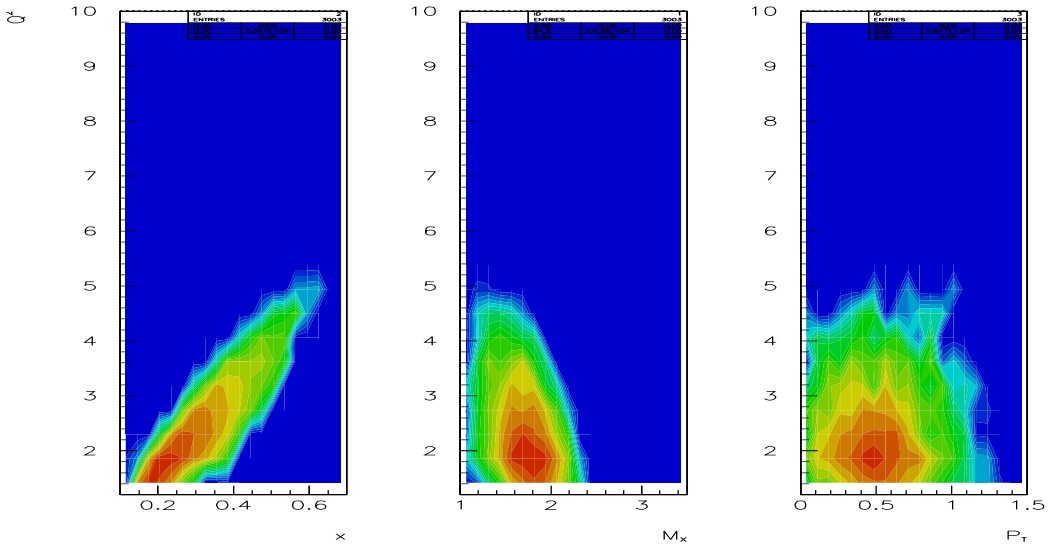

Figure 7: The SIDIS kinematic coverage in Q^2, x, M_X and P_T.

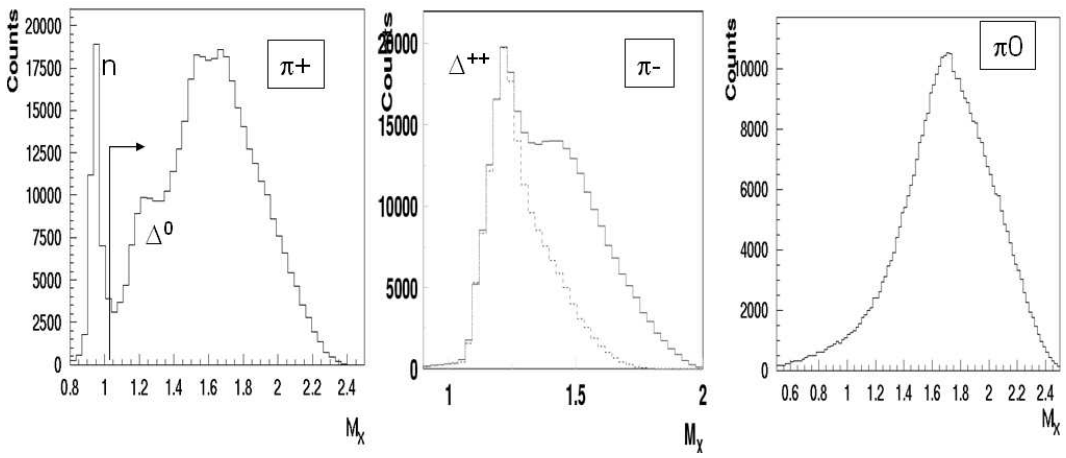

Figure 8: Missing mass distributions for pions.

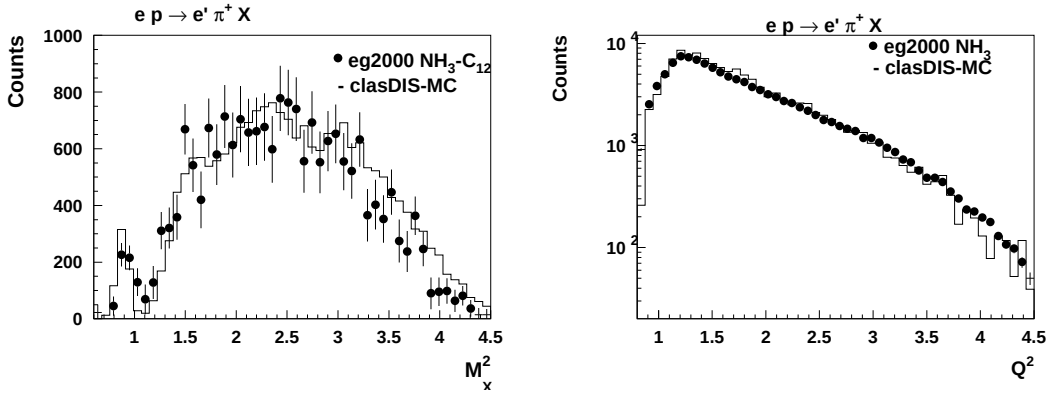

Figure 9: The M_X (left panel) and Q^2 (right) distributions from CLAS longitudinally polarized target data and PEPSI-MC.

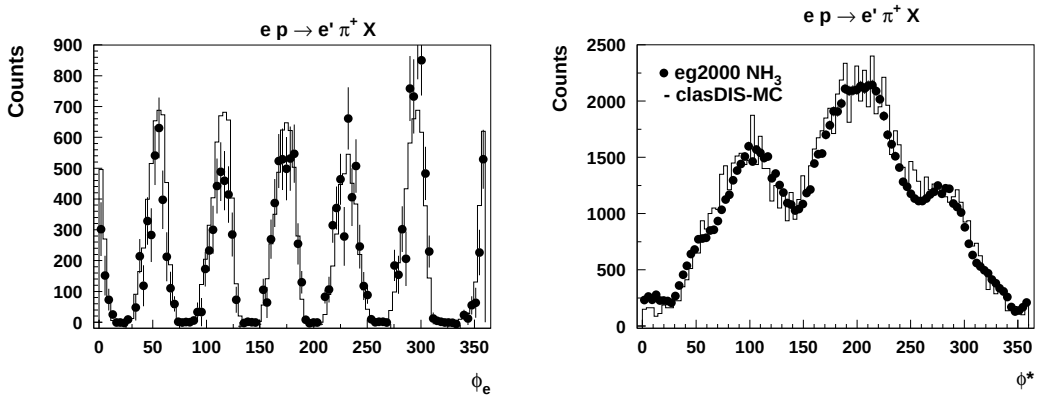

Figure 10: The Lab electron, ϕ_e, (left panel) and center of mass pion, ϕ, (right panel) azimuthal angle distributions of $e\pi^+X$ events from CLAS longitudinally polarized target data and PEPSI-MC.

3 Experimental situation

3.1 The HERMES and COMPASS Experiments

Target spin asymmetries have been published by the HERMES Collaboration on the proton [38] and COMPASS collaboration on deuterium targets [39]. Kinematics at HERMES and in particular at COMPASS is limited to relatively low x where the spin-orbit correlations are not expected to be large. The final published results from both experiments are shown along with the projected errors for this proposal on the figures in Section 4.

3.2 JLab proposals

At Jefferson Lab there is one closely-related proposal approved to measure SSA with a transversely polarized target: the Hall-A proposal on ^{3}He [82]. The data from this experiment is complementary to the proposed CLAS measurement with transversely polarized hydrogen and deuterium targets. The large acceptance of CLAS will allow measurements of SIDIS pions over a wide kinematic range including large hadron transverse momenta, where the spin-orbit correlations and corresponding TTSAs are expected to be significant. Wide acceptance and the capability to measure multi-particle final states will allow measurements of SIDIS pions and simultaneous measurements of different exclusive vector mesons, important for understanding the background contributions to the Collins and Sivers asymmetries.

The planned Hall-C SANE experiment on hydrogen [83] to study inclusive DIS has some overlap with the present proposal, but focuses on a higher average value of Q^2, and does not include SIDIS measurements.

4 A dedicated SIDIS experiment with a transversely polarized target and CLAS

The main goal of the proposed experiment is to measure the x and P_T, dependences of the target single spin asymmetries (TTSA or A_{UT}) in accessible kinematics (see Figure 7).

The target single spin asymmetry (target SSA or A_{UT}) will be calculated as:

$$A_{UT} \;=\; \frac{1}{f P_t}\frac{(N^+ \;-\; N^-)}{(N^+ \;+\; N^-)} \tag{14}$$

where P_t is the target polarization, the dilution factor f is the fraction of events from the polarized material of interest (H or D), and $N^{+(-)}$ are the charge-normalized extracted number of $ep^{\uparrow} \;\rightarrow\; e\pi X$ events for opposite orientations of the transverse spin of the target.

We will also obtain the double spin asymmetry (TDSA or A_{LT}) for the same Q^2 bins. These quantities are directly sensitive to the model descriptions of corresponding TMDs. This experiment will provide statistically significant measurements of the kinematic dependences of the target TTSA and the TDSA in the pion SIDIS in the valence region.

A_{UT} will be measured as defined in Eq. 14 and A_{LT} will be measured as:

$$A_{LT} = \frac{1}{f P_B P_t} \frac{\left(N^{+\uparrow} + N^{-\downarrow}\right) - \left(N^{+\downarrow} + N^{-\uparrow}\right)}{\left(N^{+\uparrow} + N^{-\downarrow}\right) + \left(N^{+\downarrow} + N^{-\uparrow}\right)} \tag{15}$$

where P_B is the electron beam polarization, and $N^{\pm\uparrow\downarrow}$ is the extracted number of $e\pi X$ events for positive or negative helicities of the beam electrons and target polarizations.

4.1 The CLAS configuration

4.1.1 CLAS HD Ice transversely polarized target

The magnetic holding fields accompanying transversely polarized targets can deflect the electron beam and create challenging background conditions. A magnetic chicane is typically installed upstream of the target and arranged in such a way that the target's magnetic field bends the electron beam back on axis [3]. However, bremsstrahlung created in the target material will be peaked along the direction of the incoming electrons, which will then be at several degrees to the detector axis depending on the holding field.

Generally, one can arrange to have either the electron beam or the target bremsstrahlung centered at 0^o, but not both. A transversely polarized target in a frozen-spin state, such as the HD-Ice target, requires only small holding fields, and greatly mitigates such background problems. Problems associated with beam deflection are virtually eliminated by the small holding fields and this potentially allows the target to be located even in the center of the detector, thus dramatically increasing the acceptance. In addition, the HD-Ice target has almost no dilution. The only unpolarizable nucleons are associated with the target cell and these can be sampled and subtracted in conventionally empty-cell measurements. At the same time, the low Z results in a long radiation length and comparatively few bremsstrahlung photons.

The HD-Ice target developed at LEGS in Brookhaven and now being moved from BNL to JLab, has been used quite successfully in photon beam experiments. The factors affecting target polarization are complex and intertwined; a direct test of the performance of polarized HD with electrons is essential. This will be carried out during the course of the E06-101 run [84].

At BNL, HD target polarizations of 60% H and 35% D have been used in photon experiments with spin-relaxation times in excess of a year, and polarizations are expected to be higher (75% H and 40% D) with the smaller diameter cells that will

be used at JLab. The deuterium polarization is particularly stable; spin-relaxation times of 2 months have been measured with only 0.01 T (100 gauss) holding field and 0.2 K. The projected D-decay time for a 0.04 T saddle coil, 0.12 m in length ($BdL \approx$ 0.005 T-m), is 7 months. Comparable H relaxation times require higher fields but should be possible with $BdL = 0.050$ T-m, which is still about 30 times less than a dynamically polarized ammonia target. The beam heating expected from 5 nA of 6 GeV electrons traversing a 4 cm HD target is $\sim$ 10 mW (as calculated with GEANT). This is about the cooling power of the existing BNL In-Beam-Cryostat (IBC) at 0.5 K and will be significantly increased in the CLAS-IBC now under design for E06-101. Beam heating is considerably less in HD, as compared to Butanol, due to the lower Z and, unlike butanol, HD relaxation times are not such strong functions of temperature so that long life-times are achievable up to about 0.7 K. Free radicals generated by electron bremsstrahlung will have randomly oriented polarizations. While their absolute number is small, they can generate polarization sinks within the target if the spin-diffusion time is short. This time constant has been indirectly measured at BNL by using RF to punch a local polarization hole within a highly polarized target. The rate at which this hole heals after the RF power is lowered reflects the in-diffusion of spin from other regions of the target. At 2 K, this measured spin-diffusion is 1 day for H but unmeasurably long for D (greater than a year). How much the H performance improves at lower temperatures is a matter for further study, but the extremely slow spin-diffusion for D already suggests that frozen-spin HD could maintain its deuterium polarization during electron experiments. The composition for a 4 cm HD-Ice target is shown in the Table 4.1.1

Table 2: HD-Ice materials.

Material	gm/cm^2	mass fraction (%)
HD	0.735	77%
Al	0.155	16%
CTFF	0.065	7%

Frozen-spin HD-Ice, thus, provides a very attractive alternative for electron experiments in particular with transversely polarized targets.

4.1.2 Beam rastering

To avoid radiation damage to the target the beam will be rastered over the target surface in a spiral pattern. The beam position is measured indirectly by recording the simultaneous currents of the raster magnet. These values can be used off-line to correct for effects of the raster on the vertex z-position. Figure 11 shows the z-vertex position before and after correction for polarized target data set.

The raster magnets may be also used to give a small angle ($\sim 0.2^o$) to the incident electron beam, so that beam at target center will be collinear with the z-axis to confine

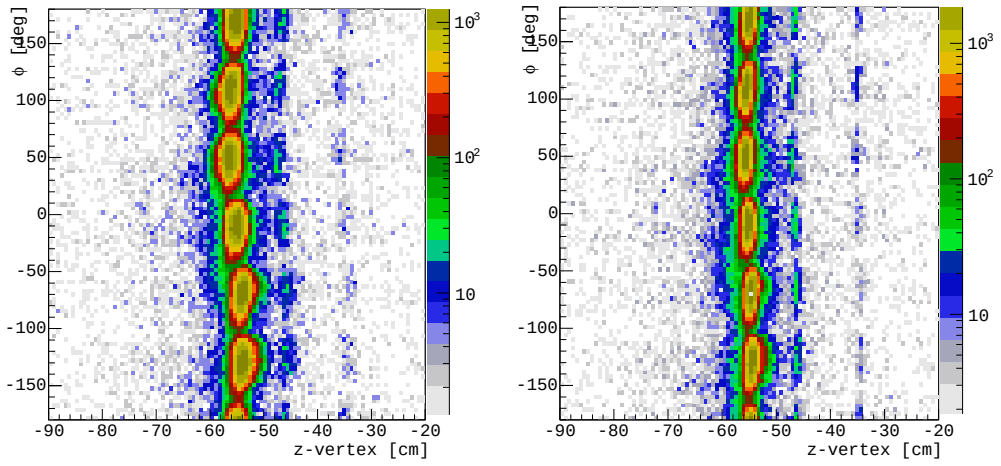

(a) original (b) corrected

Figure 11: Electron z-vertex position for EG1b data before and after the raster corrections

bremsstrahlung photons in the beam pipe. The deflection of the primary beam by the target field will be fixed by a compensation coil or upstream magnets located in region III of CLAS. Figure 12 shows the CLAS setup with transversely polarized target at z=-70 cm and minitorus at z=-50 cm.

4.1.3 Minitorus magnet as magnetic shield

One of the main sources of background produced by a high-energy electron beam impinging upon a HD target is due to interactions of the electron beam with the atomic electrons (Møller scattering). This rate is several orders of magnitude larger than the inelastic hadronic production rate. The CLAS minitorus magnet will be used to focus Møller electrons, so they will be absorbed in the downstream shielding pipe (Fig. 12).
The relative position of the minitorus and the target with respect to the CLAS center will be optimized using the GSIM. The background rates due to Møller electrons are relatively small due to low density of the target and low current, which will be mainly limited by the target capability to keep the polarization.

Locating the target upstream will significantly increase the kinematic coverage for the high momentum π^0s. The reconstruction efficiency as a function of the azimuthal angle ϕ and transverse momentum P_T is shown in Fig. 13 for all 3 pions.

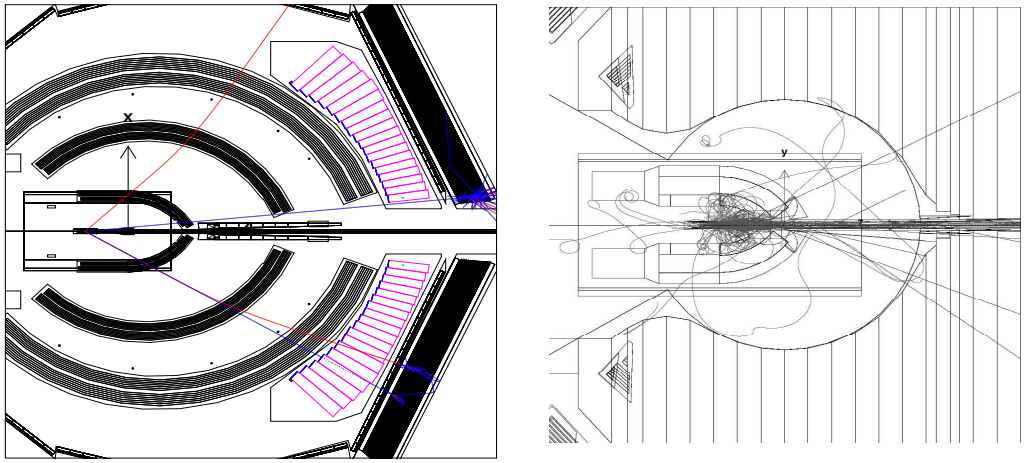

Figure 12: CLAS setup with HD-Ice target positioned at -70 cm. Minitorus positioned at -50 cm. A single event shown in CLAS (left) and Moller electrons in the field of minitorus (right)

4.1.4 Target polarization measurements

There are four possible transverse combinations: (1) H and D both up, (2) H up/D down, (3) H down/D up, (4) H and D both down. Using the RF flipping of spins, one can switch between (1) and (4) or between (2) and (3) by simply rotating the field. The spins will follow, and this has 100% efficiency. Several samples with different orientations will be used in the experiment.

The target polarization will be measured with an NMR system [84, 85, 86]. Polarimetry for nuclear targets has been studied extensively at BNL. The In-Beam-Cryostat that will hold HD targets within the CLAS will have a short saddle coil wound on top of a long solenoid. The saddle coil will maintain transverse spin orientations. Keeping this coil short will both reduce the BdL deflection of electrons as well as minimize spin diffusion from radiation damage (by changing the Larmor frequency across the target). However, the fields associated with this coil will be too non-uniform for NMR measurements. Instead, the solenoid will be used for NMR polarization monitoring. The target spins will readily follow the field as the solenoid is energized and the saddle coil is ramped down. NMR data will be collected at the fields matching the Larmor frequencies, typically 0.15 T for H and 0.9 T for D, after which the saddle coil will be ramped up and the solenoid ramped down. We anticipate a total cycle time of about 15 minutes (limited by how fast fields can be changed without quenching the magnets), enabling NMR data to be collected several times a day. The systematic uncertainties in HD polarization are about 4% (relative). The largest single factor (contributing 2.8% relative) is the differential uncertainty on the gain of a lock-in amplifier whose scale must be changed by many orders of magnitude between equilibrium-polarization measurements and high-polarization frozen-spin measurements. Separation of signal and background in the calibration

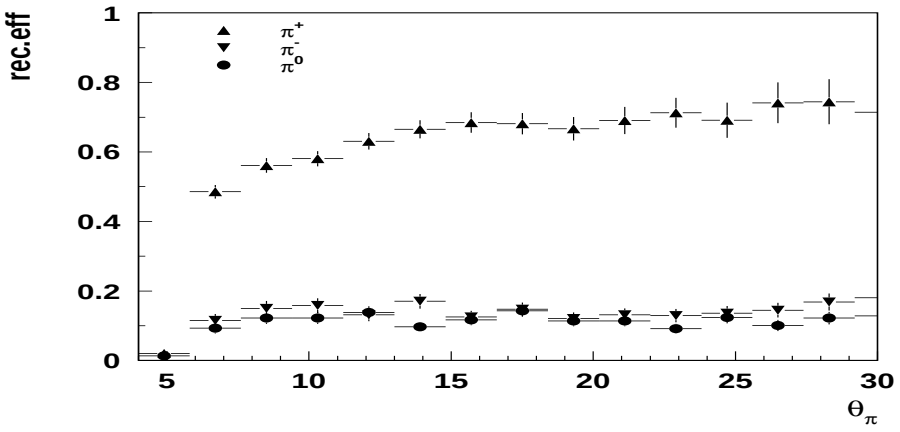

Figure 13: The reconstruction efficiency of SIDIS pions ($e\pi X$ sample) for $Q^2 > 1.5$ as a function of the pion polar angle.

measurements contributes at the 1% level.

Additional estimate of the product of target and beam polarizations, $P_B P_t$, will be done also off-line by comparing the well known ep elastic asymmetry

$$A_{theo} = -\frac{\cos\theta_\gamma\sqrt{1-\epsilon^2} + (\frac{Q^2}{4M^2})^{-\frac{1}{2}}\sqrt{2\epsilon(1-\epsilon)}\sin\theta_\gamma\cos\phi_\gamma\frac{G_E}{G_M}}{\epsilon(\frac{Q^2}{4M^2})^{-1}(\frac{G_E}{G_M})^2 + 1} \tag{16}$$

with the measured asymmetry

$$A_{meas} = \frac{N^+ - N^-}{N^+ + N^-} = \frac{P_B P_t \sigma_{et}}{\sigma_0} \equiv P_B P_t A_{theo}. \tag{17}$$

For the ratio $\frac{G_E}{G_M}$, we will use values from polarization transfer measurements [87], which are expected theoretically to have the same (small) two-photon corrections as A_{LT} measurements. On average, the uncertainty in A_{LT} due to G_E/G_M will be about 2% (relative). The measurements will consist of measuring both an electron and a proton, and imposing missing momentum and energy cuts to isolate the elastic channel. Events from H and D will be distinguished through a multi-parameter fit to the missing mass and energy distributions: Fermi broadening in the deuteron generates peaks that are typically twice as wide as for hydrogen, for the conditions of this proposal (based on the similar conditions in EG1). Due to this mixing, the errors will be approximately 1.4 times bigger than for targets which contain only H

or D plus heavy materials such as nitrogen or aluminum. The projected errors on A_{LT} for H from this experiment are shown in Fig. 15. For comparison, the larger A_{LL} asymmetries measured in EG1 at 5.7 GeV are also shown. Averaged over Q^2, we expect to determine the product of beam and target polarization, $P_B P_t$, with a relative statistical precision of 3%, and s systematic error of 2%. For the deueron, we project errors of 7% atatistical and 4% systematic. The larger systematic error, relative to the proton, is driven by quasi-elastic modeling uncertainties.

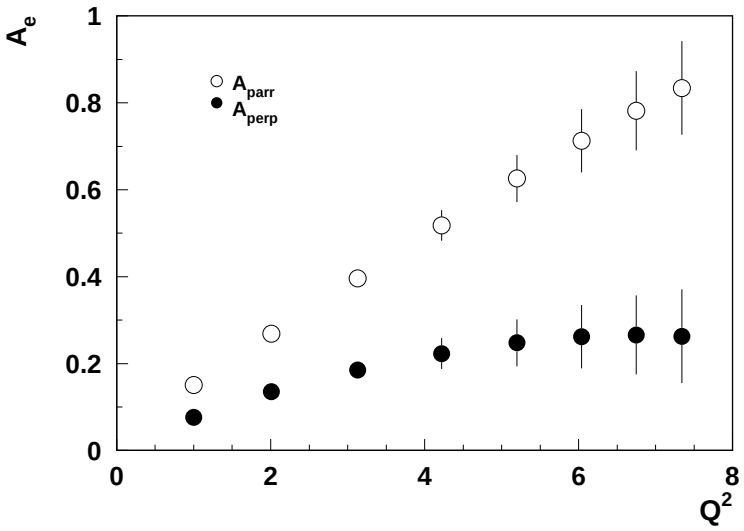

Figure 14: Projected *ep* elastic asymmetry A_{LT} and corresponding errors for H for this proposal as a function of Q^2 (solid circles). For comparison, A_{LL} asymmetries from EG1 are also shown.

The beam polarization will be measured periodically with the standard Hall-B Moller polarimeter.

4.1.5 Trigger and data acquisition

We are planning to use the standard e1 production trigger, data acquisition, and online monitoring system of CLAS. The signal amplitude and time information will be read out using standard ADC and TDC boards currently in use in CLAS. The standard CLAS level 1 trigger will be used to select scattered electrons. No changes to the trigger hardware are anticipated. Run conditions including the torus field (2250 A) will be similar to the e1f run period.

4.2 Event identification, reconstruction, and acceptances

Standard CLAS particle ID will be used for event identification for $ep^{\uparrow} \rightarrow e\pi X$ in CLAS, where final-state pion and scattered electron will be detected. Electrons are separated from heavier particles using threshold gas Cherenkov counters (CC) and electromagnetic calorimeters, and pions are identified using tracking in the toroidal magnetic field and measurement of time of flight. Pion momenta are reconstructed in the CLAS drift chamber system using the standard CLAS reconstruction software. For the proposed experiment, photons from π^0 decays (or from η decays) will be reconstructed using the CLAS forward angle electromagnetic calorimeter (EC). The shifted upstream target will provide large acceptance coverage for both reactions.

4.3 Acceptance and data analysis

Although SSAs typically are not too sensitive to acceptance corrections, in the case of the transverse target, due to large number of contributions appearing as different azimuthal moments in the cross section, acceptance corrections are more important. The analysis of the transverse target requires fits in 2 dimensional space of relevant azimuthal angles ϕ and ϕ_S. A detailed procedure on accounting for acceptance corrections in separation of different azimuthal moments was developed by the HERMES collaboration [38]. A similar procedure will be applied, to estimate expected acceptance corrections for Sivers and Collins asymmetries using the CLAS acceptance.

4.4 Count rates and statistical errors

The expected number of counts is given by

$$N = \mathcal{L} \times \text{time} \times \sigma \times (\Delta Q^2 \cdot \Delta x_B) \times \Delta z \times \Delta P_T \times \Delta\phi \times (\Delta\varphi_e)_{\text{eff}}/2\pi \qquad (18)$$

With the proposed configuration as described in Sec. 4.1, a luminosity of 5×10^{33} $\text{cm}^{-2}\text{s}^{-1}$ is expected.

The resulting number of SIDIS pion events for the proposed experiment is calculated from the 5 days of the EG1 run at 5.7 GeV, scaled to 25 days for hydrogen and reduced by a factor of four less luminosity. The total number of SIDIS pions from EG1, in similar kinematic conditions within cuts $Q^2 > 1$ GeV^2, $W > 2$ GeV, $M_X > 1.4$ GeV, $0.4 < z < 0.7$ was 2144k, 1278k, 815k for π^+, π^- and π^0, respectively.

The target polarization is assumed 75% for hydrogen (25% for deuterium) and 40% for deuterium (none for hydrogen), so 25 days with polarized hydrogen and 15 days with polarized deuterium will provide comparable statistical error bars. We plan to have 5 days of calibration runs, including measurements with frozen H, D, and empty targets. The beam polarization of 0.85 is assumed for the calculation of $\Delta(TDSA)$. The dilution factor f is more than a factor of two larger for the present proposal than for EG1b. All the above factors have been taken into account when calculating the statistical uncertainties on the asymmetries.

4.5 Systematic errors

The systematic errors can be divided into two categroies: those that scale with the measured asymmetry, and those that are independent of the measured results. In the first category, the dominant eror is expected to be that from target polarization and the dilution from the unwanted HD and Al backgrounds. For the second catagory, we have taken our best estimate of the magnitude of the systematic effect, and divided by the average expected proton asymmetry. One of the main contributions to the estimated relative uncertainties, summarized in Table 4.5, comes from the procedure used to separate the aizimuthal moments of interest from other, potentially non-zero, azimuthal asymmetries (for example a twist-3 $\sin(\phi_S)$ moment). Another large contribution is from possible contamination of the SIDIS pion event sample by pions from decays of diffractive vector mesons, mainly ρ^0. Thanks to the large acceptance of CLAS, the asymmetries from background processes such as ρ^0 production will be measured simultaneously and can thus be corrected for, as the size of the contamination can be measured as well. Based on our previous studies for the EG1, e1f and e16 experiments, the uncertainty from radiative corrections will be small.

We conservatively estimate the average total relative systematic error on the proton SSAs to be of order 10%, sufficiently small for a very significant measurement.

Table 3: Estimated contributions to the relative systematic uncertainty on the proton TTSAs in SIDIS.

Error source	Systematic error (%)
H/D background	4
P_T	5
acceptance corrections	6
Al background contribution	3
ρ^0 contamination	5
Radiative corrections	3
Total	~ 10

4.6 Projected results

4.6.1 TMD measurements

The corresponding projections for CLAS data set based on 40 days of production runs with HD-Ice target are shown in Fig. 15 and Fig. 16 respectively, for different approximations for Sivers function.

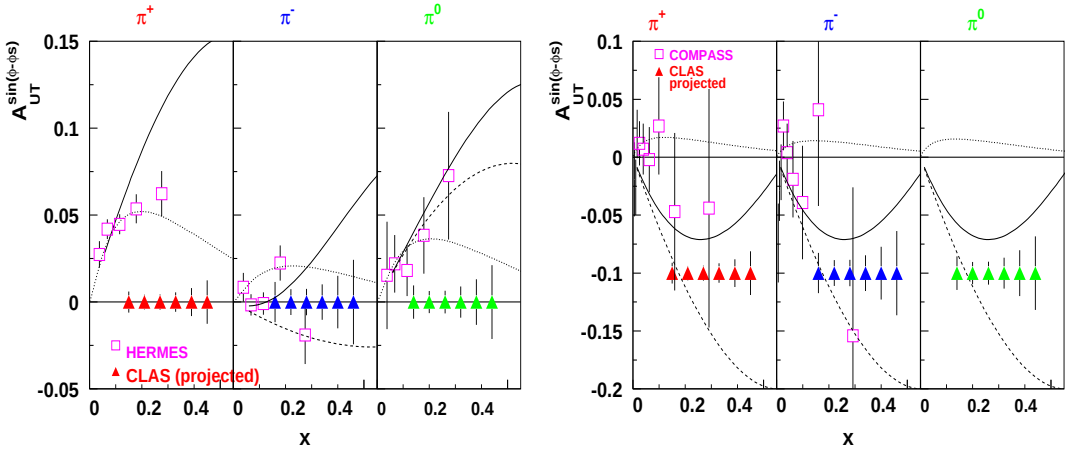

Figure 15: Expected Sivers TTSA $A_{UT}^{\sin(\phi-\phi_S)}$ as a function of x. The projected statistical error for hydrogen target (left) and deuterium target (right) is shown. Curves were calculated using two parameterizations from Ref.[88] (solid and dashed) and Ref.[89, 90] (dotted). The systematic error is expected to not exceed the statistical one.

Parameterization used are fits to existing HERMES and COMPASS data at small x. Precision measurements at CLAS will help to constrain different models, in particular for the deuteron part (Fig.15). The measurement of the transverse asymmetry from the Sivers effect with π^0 will provide a model-independent extraction of the Sivers function in the large-x region, where the sea contribution is not significant. Furthermore, measurements with proton and neutron targets will provide model-independent information on flavor partners of the Sivers function.

Projections for the Collins asymmetry are shown in Fig.17, indicating that CLAS can make important contribution also in transversity measurements in the valence region. Proposed measurements of SSAs in SIDIS will constrain the corresponding TMD distributions and provide information on the ratio of favored to unfavored polarized fragmentation functions, complementary to e^+e^- data.

Superior beam polarization at JLab ($P_B \approx 85\%$) provides access to double spin asymmetry measurements with the transversely polarized target. The variation of the

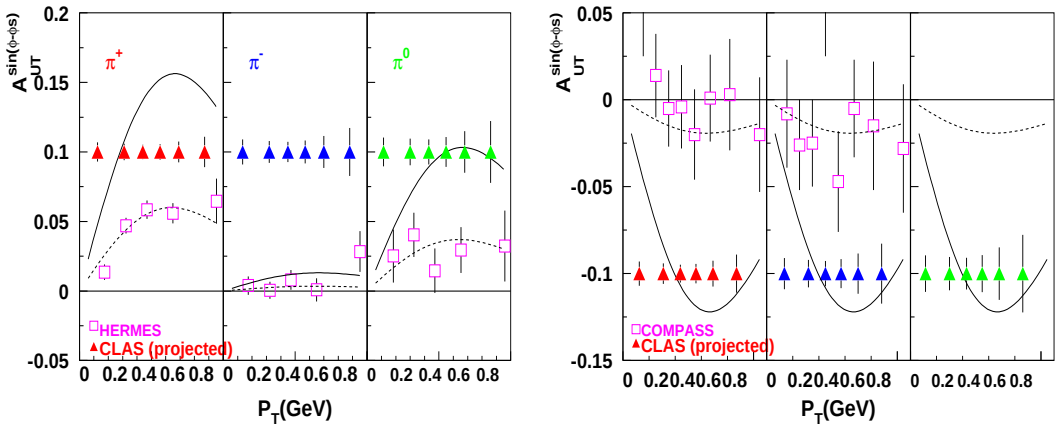

Figure 16: Expected Sivers TTSA $A_{UT}^{\sin(\phi-\phi_S)}$ as a function of P_T The projected statistical error for 25 polarized hydrogen (left) and deuteron (right) targets is shown. Curves were calculated for CLAS (solid line) and HERMES/COMPASS kinematics (dashed line) using the parameterization for Sivers function from Ref.[88], using a Gaussian distribution in k_T [91]. The systematic error is expected to not exceed the statistical one.

double spin asymmetries (TDSA) as a function of the relevant kinematic variables according to different TMD models are shown in Fig.18

4.6.2 Inclusive measurements

The projected error bars on g_2 for both targets are shown as a function of x for several bins in Q^2 in Fig. 19. The "cross" symbols correspond to kinematics where the Hall C RSS experiment [92] has already taken data ($Q^2 = 1.3$ GeV^2, $x > 0.3$), with errors similar to those from the present proposal. The crosses also indicate some overlap with the upcoming SANE experiment [93] in Hall C, which uses a proton target only, a 6 GeV electron beam and scattering angles $32 < \theta < 48$ degrees. The present proposal will provide a valuable confirmation of the RSS and SANE results, and significantly extend the available (x, Q^2) range of precision data, especially for the deuteron. The g_2 measurements on both the proton and deuteron from SLAC [94] are at larger average values of Q^2 than the present proposal, for a given value of x. Although the error bars from SLAC are typically a factor of two larger than those from this proposal, the proton errors will be reduced significantly the SANE experiment [93]. Combining the results of all experiments together with the present proposal results will generate a definite set of measurements of g_2 for both the proton

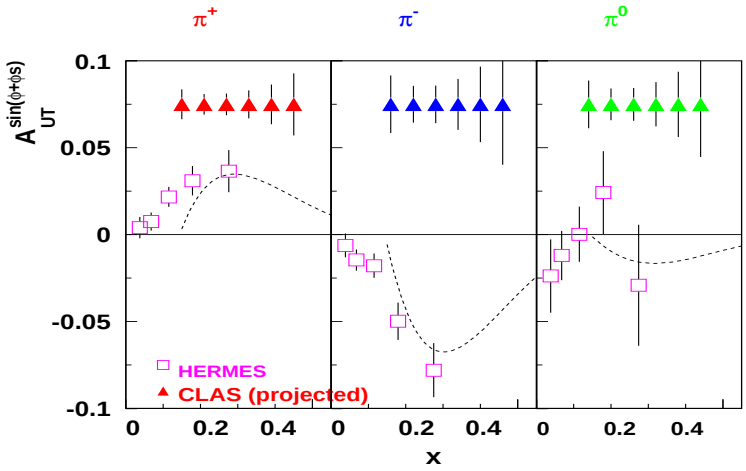

Figure 17: Expected Collins TTSA $A_{UT}^{\sin(\phi+\phi_S)}$ as a function of x_B. The projected statistical error for proton target is shown. Curves represent predictions for CLAS kinematics from Ref.[63]. The systematic error is expected to not exceed the statistical one.

and neutron, allowing precise determinations of QCD-calculable moments such as $\bar{d}_2$, $\gamma_0(Q^2)$, and δ_{LT} over a wide range in Q^2: $0.5 < Q^2 < 5$ GeV^2.

0 0.5 0 0.5 0 0.5

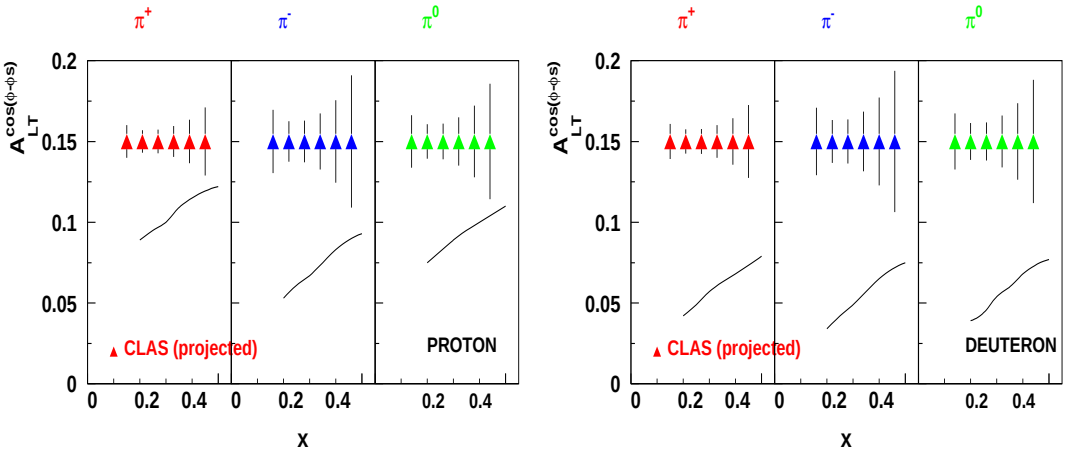

Figure 18: Expected double spin asymmetry TDSA $A_{LT}^{\cos(\phi-\phi_S)}$ as a function of x The projected statistical error for transversely polarized proton(left) and deuteron (right) targets is shown. Curves correspond to calculations for proton and deuteron targets from Ref.[70]. The beam polarization was assumed 85%. The systematic error is expected to not exceed the statistical one.

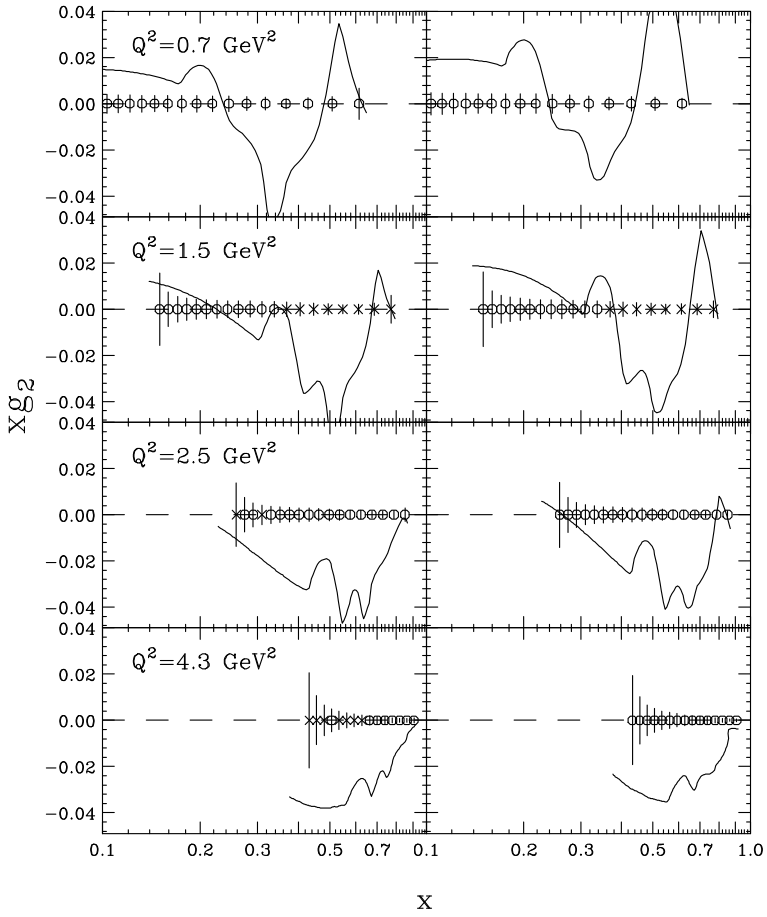

Figure 19: Projected errors for xg_2 from this proposal as a function of x in four bins in Q^2 for proton (left) and deuteron (right). The "cross" symbol is used for kinematic settings that overlap with Hall C experiments RSS or SANE. The curves are a from the g_2 model used in the analysis of Hall B experiment Eg1b.

5 Summary and beam time request

In this experiment we propose a study of the Transverse Momentum Dependent (TMD) parton distributions via measurements of pion production in SIDIS in the hard scattering kinematics ($Q^2 > 1\text{GeV}^2$, $W^2 > 4\text{GeV}^2$), using a 6 GeV electron beam and the CLAS detector. The experiment will use CLAS with the transversely polarized HD-Ice target located upstream. Increased, compared to regular runs with mini-torus (e16 and e1f), acceptance for high energy π^0s (>50%, variable with kinematics), will allow us to extend to large-x measurements of neutral pion SSAs with transversely polarized hydrogen and deuterium targets. For this proposal, we request 45 days of beam time with high polarization of electrons at 6 GeV and a transversely polarized hydrogen and deuteron targets (40 days of production runs and 5 for calibration). We expect to improve statistical uncertainties of HERMES (~ 4) measurements on hydrogen and COMPASS (~ 8) on deuterium at large x (x >0.2). The CLAS data covering large transverse momentum of pions, will also be crucial in interpretation of the Hall-A experiment on the ^{3}He target.

The large acceptance of the CLAS detector permits a simultaneous scan of various variables (x_B, z, P_T and ϕ), so large acceptance detector such as CLAS is most suitable. Analysis of already existing electro-production data from CLAS with unpolarized and longitudinally polarized targets have shown that the proposed measurements are feasible. Combined analysis of all three data sets will constrain different TMDs and relations between them, providing important input to global analysis of 3D PDFs, also helping to maintain the momentum in the theory community.

Beam Request

We ask the PAC to award 45 days of beam time for a dedicated high statistics SIDIS experiment with the transversely polarized target.

Approximately ten calendar days will be needed for configuration changes. No new equipment is involved and the experiment could be ready after tests with HD-Ice target will verify polarization retention with electron beam. The measurements involve the standard CLAS configuration also proposed for DVCS studies [53]. Therefore these experiments can run simultaneously.

The measurement will produce precise data on underlying quark transverse momentum distributions, providing important information on spin-orbit correlations. The focus here is on higher-order corrections which likely will be important for a complete understanding of the expected results from the proposed measurement and future measurements with CLAS12. Understanding of spin-orbit correlations together with independent measurements related to spatial distributions and orbital angular momentum will help to construct a more complete picture of the nucleon in terms of

elementary quarks and gluons going beyond the simple collinear partonic representation.

References

[1] European Muon, J. Ashman et al., Phys. Lett. B206 (1988) 364.

[2] Spin Muon (SMC), D. Adams et al., Phys. Rev. D56 (1997) 5330, hep-ex/9702005.

[3] E143, K. Abe et al., Phys. Rev. D58 (1998) 112003, hep-ph/9802357.

[4] E155, P.L. Anthony et al., Phys. Lett. B458 (1999) 529, hep-ex/9901006.

[5] HERMES, K. Ackerstaff et al., Phys. Lett. B464 (1999) 123, hep-ex/9906035.

[6] HERMES, A. Airapetian et al., Phys. Rev. D71 (2005) 012003, hep-ex/0407032.

[7] CLAS, R. Fatemi et al., Phys. Rev. Lett. 91 (2003) 222002, nucl-ex/0306019.

[8] S.J. Brodsky, D.S. Hwang and I. Schmidt, Phys. Lett. B530 (2002) 99, hep-ph/0201296.

[9] J.C. Collins, Phys. Lett. B536 (2002) 43, hep-ph/0204004.

[10] X. Ji and F. Yuan, Phys. Lett. B543 (2002) 66, hep-ph/0206057.

[11] A.V. Belitsky, X. Ji and F. Yuan, Nucl. Phys. B656 (2003) 165, hep-ph/0208038.

[12] D. Boer, S.J. Brodsky and D.S. Hwang, Phys. Rev. D67 (2003) 054003, hep-ph/0211110.

[13] D. Boer, P.J. Mulders and F. Pijlman, Nucl. Phys. B667 (2003) 201, hep-ph/0303034.

[14] X. Ji, J. Ma and F. Yuan, Phys. Rev. D71 (2005) 034005, hep-ph/0404183.

[15] J.C. Collins and A. Metz, Phys. Rev. Lett. 93 (2004) 252001, hep-ph/0408249.

[16] X. Ji, J.P. Ma and F. Yuan, Nucl. Phys. B652 (2003) 383, hep-ph/0210430.

[17] D.W. Sivers, Phys. Rev. D43 (1991) 261.

[18] D. Boer and P.J. Mulders, Phys. Rev. D57 (1998) 5780, hep-ph/9711485.

[19] M. Anselmino and F. Murgia, Phys. Lett. B442 (1998) 470, hep-ph/9808426.

[20] S.J. Brodsky, D.S. Hwang and I. Schmidt, Nucl. Phys. B642 (2002) 344, hep-ph/0206259.

[21] M. Burkardt, Phys. Rev. D72 (2005) 094020, hep-ph/0505189.

[22] M. Gockeler et al., Nucl. Phys. Proc. Suppl. 153 (2006) 146, hep-lat/0512011.

[23] QCDSF, M. Gockeler et al., Phys. Rev. Lett. 98 (2007) 222001, hep-lat/0612032.

[24] J.C. Collins, Nucl. Phys. B396 (1993) 161, hep-ph/9208213.

[25] A.V. Efremov, K. Goeke and P. Schweitzer, Phys. Rev. D67 (2003) 114014, hep-ph/0208124.

[26] A. Afanasev and C.E. Carlson, (2003), hep-ph/0308163.

[27] F. Yuan, Phys. Lett. B589 (2004) 28, hep-ph/0310279.

[28] A. Metz and M. Schlegel, Eur. Phys. J. A22 (2004) 489, hep-ph/0403182.

[29] HERMES, A. Airapetian et al., Phys. Rev. Lett. 84 (2000) 4047, hep-ex/9910062.

[30] HERMES, A. Airapetian et al., Phys. Rev. D64 (2001) 097101, hep-ex/0104005.

[31] HERMES, A. Airapetian et al., Phys. Lett. B562 (2003) 182, hep-ex/0212039.

[32] HERMES, A. Airapetian et al., Phys. Lett. B648 (2007) 164, hep-ex/0612059.

[33] CLAS, H. Avakian et al., Phys. Rev. D69 (2004) 112004, hep-ex/0301005.

[34] A. Bacchetta, P.J. Mulders and F. Pijlman, Phys. Lett. B595 (2004) 309, hep-ph/0405154.

[35] K. Goeke, A. Metz and M. Schlegel, Phys. Lett. B618 (2005) 90, hep-ph/0504130.

[36] on behalf of the COMPASS, A. Kotzinian, (2007), arXiv:0705.2402 [hep-ex].

[37] COMPASS, P. Abbon et al., Nucl. Instrum. Meth. A577 (2007) 455, hep-ex/0703049.

[38] HERMES, A. Airapetian et al., Phys. Rev. Lett. 94 (2005) 012002, hep-ex/0408013.

[39] COMPASS, V.Y. Alexakhin et al., Phys. Rev. Lett. 94 (2005) 202002, hep-ex/0503002.

[40] J.P. Ralston and D.E. Soper, Nucl. Phys. B152 (1979) 109.

[41] R.L. Jaffe and X. Ji, Nucl. Phys. B375 (1992) 527.

[42] X.d. Ji, J.P. Ma and F. Yuan, Phys. Lett. B597 (2004) 299, hep-ph/0405085.

[43] P.J. Mulders and R.D. Tangerman, Nucl. Phys. B461 (1996) 197, hep-ph/9510301.

[44] A. Kotzinian, Nucl. Phys. B441 (1995) 234, hep-ph/9412283.

[45] A.M. Kotzinian and P.J. Mulders, Phys. Rev. D54 (1996) 1229, hep-ph/9511420.

[46] E. Leader, A.V. Sidorov and D.B. Stamenov, Phys. Lett. B462 (1999) 189, hep-ph/9905512.

[47] H.C. Kim, M.V. Polyakov and K. Goeke, Phys. Lett. B387 (1996) 577, hep-ph/9604442.

[48] D. Mueller et al., Fortschr. Phys. 42 (1994) 101, hep-ph/9812448.

[49] X.D. Ji, Phys. Rev. D55 (1997) 7114, hep-ph/9609381.

[50] X.D. Ji, Phys. Rev. Lett. 78 (1997) 610, hep-ph/9603249.

[51] A.V. Radyushkin, Phys. Lett. B380 (1996) 417, hep-ph/9604317.

[52] M. Burkardt, Int. J. Mod. Phys. A18 (2003) 173, hep-ph/0207047.

[53] Hall-B, . H.Avakian et al., CLAS proposal to study DVCS with transversely polarized target (2007).

[54] M. Diehl and P. Hagler, Eur. Phys. J. C44 (2005) 87, hep-ph/0504175.

[55] S. Meissner, A. Metz and K. Goeke, Phys. Rev. D76 (2007) 034002, hep-ph/0703176.

[56] M. Burkardt and D.S. Hwang, Phys. Rev. D69 (2004) 074032, hep-ph/0309072.

[57] Z. Lu and I. Schmidt, Phys. Rev. D75 (2007) 073008, hep-ph/0611158.

[58] G.A. Miller, (2007), arXiv:0708.2297 [nucl-th].

[59] M. Burkardt, (2007), arXiv:0709.2966 [hep-ph].

[60] A. Bacchetta et al., Phys. Rev. D65 (2002) 094021, hep-ph/0201091.

[61] A.M. Kotzinian et al., (1999), hep-ph/9908466.

[62] Belle, K. Abe et al., Phys. Rev. Lett. 96 (2006) 232002, hep-ex/0507063.

[63] M. Anselmino et al., Phys. Rev. D75 (2007) 054032, hep-ph/0701006.

[64] COMPASS, B. Parsamyan, (2007), arXiv:0709.3440 [hep-ex].

[65] H. Avakian et al., Phys. Rev. Lett. 99 (2007) 082001, arXiv:0705.1553 [hep-ph].

[66] X. Ji et al., Phys. Rev. D73 (2006) 094017, hep-ph/0604023.

[67] J.w. Qiu and G. Sterman, Phys. Rev. Lett. 67 (1991) 2264.

[68] E581, D.L. Adams et al., Z. Phys. C56 (1992) 181.

[69] STAR, J. Adams et al., Phys. Rev. Lett. 92 (2004) 171801, hep-ex/0310058.

[70] A. Kotzinian, B. Parsamyan and A. Prokudin, Phys. Rev. D73 (2006) 114017, hep-ph/0603194.

[71] R.L. Jaffe, Int. J. Mod. Phys. A18 (2003) 1141, hep-ph/0201068.

[72] CLAS, H. Avakian et al., AIP Conf. Proc. 792 (2005) 945, nucl-ex/0509032.

[73] H. Mkrtchyan et al., (2007), arXiv:0709.3020 [hep-ph].

[74] R.L. Jaffe and X.D. Ji, Phys. Rev. D43 (1991) 724.

[75] M. Gockeler et al., Phys. Rev. D53 (1996) 2317, hep-lat/9508004.

[76] M. Gockeler et al., Phys. Rev. D63 (2001) 074506, hep-lat/0011091.

[77] Jefferson Lab E94-010, M. Amarian et al., Phys. Rev. Lett. 92 (2004) 022301, hep-ex/0310003.

[78] Jefferson Lab Hall A, X. Zheng et al., Phys. Rev. C70 (2004) 065207, nucl-ex/0405006.

[79] CLAS, K.V. Dharmawardane et al., Phys. Lett. B641 (2006) 11, nucl-ex/0605028.

[80] D. Drechsel, B. Pasquini and M. Vanderhaeghen, Phys. Rept. 378 (2003) 99, hep-ph/0212124.

[81] D. Drechsel and L. Tiator, Ann. Rev. Nucl. Part. Sci. 54 (2004) 69, nucl-th/0406059.

[82] Hall-A, . X.Jiang et al., Hall-A proposal E06-010 (2006).

[83] Hall-A, . X.Jiang et al., Hall-C proposal E06-012 (2006).

[84] CLAS, . A.Sandorfi et al., CLAS proposal E06-101 (2006).

[85] A. Caracappa and C. Thorn, AIP Conf. Proc. 675 (2003) 867.

[86] C. Thorn and . Caracappa, AIP Conf. Proc. (2007) (in press).

[87] Jefferson Lab Hall A, M.K. Jones et al., Phys. Rev. Lett. 84 (2000) 1398, nucl-ex/9910005.

[88] W. Vogelsang and F. Yuan, Phys. Rev. D72 (2005) 054028, hep-ph/0507266.

[89] A.V. Efremov et al., Phys. Lett. B612 (2005) 233, hep-ph/0412353.

[90] J.C. Collins et al., Phys. Rev. D73 (2006) 014021, hep-ph/0509076.

[91] M. Anselmino et al., Phys. Rev. D74 (2006) 074015, hep-ph/0608048.

[92] RSS, F.R. Wesselmann et al., Phys. Rev. Lett. 98 (2007) 132003, nucl-ex/0608003.

[93] Hall-C, O.A. S.Choi, Z.E. Meziani et al., Hall-C proposal E-07-003 (2003).

[94] E155, P.L. Anthony et al., Phys. Lett. B553 (2003) 18, hep-ex/0204028.